

Thermoelectric transport of the half-filled lowest Landau level in a p -type Ge/SiGe heterostructure

Xiaoxue Liu¹, Tzu-Ming Lu^{2,3}, Charles Thomas Harris^{2,3}, Fang-Liang Lu^{4,5}, Chia-You Liu^{4,5}, Jiun-Yun Li^{4,5}, Chee Wee Liu^{4,5}, and Rui-Rui Du¹

¹*Rice University, Houston, Texas 77251-1892, USA*

²*Sandia National Laboratories, Albuquerque, New Mexico 87185, USA*

³*Center for Integrated Nanotechnologies, Sandia National Laboratories, Albuquerque, New Mexico, 87123, USA*

⁴*Department of Electrical Engineering and Graduate Institute of Electronic Engineering, National Taiwan University, Taipei, 10617, Taiwan, ROC*

⁵*National Nano Device Laboratories, Hsinchu, 30077, Taiwan, ROC*

Abstract

We investigate the thermoelectric transport properties of the half-filled lowest Landau level $\nu = 1/2$ in a gated two-dimensional hole system in a strained Ge/SiGe heterostructure. The electron-diffusion dominated regime is achieved below 600 mK, where the diffusion thermopower S_{xx}^d at $\nu = 1/2$ shows a linear temperature dependence. In contrast, the diffusion-dominated Nernst signal S_{xy}^d of $\nu = 1/2$ is found to approach zero, which is independent of the measurement configuration (sweeping magnetic field at a fixed hole density or sweeping the density by a gate at a fixed magnetic field).

The half-filled lowest Landau level $\nu = 1/2$ state is one of the most intriguing quantum ground states in a two-dimensional electron system under a strong magnetic field at low temperatures. Halperin-Lee-Read (HLR) theory states that composite fermions at $\nu = 1/2$ consisting of one electron and two flux quanta are effectively in a zero magnetic field [1]. Over the past two decades, HLR theory has gained great success for explaining $\nu = 1/2$ as the compressible composite fermion liquid state with a distinct Fermi surface [2-7]. However, recently HLR theory has been questioned for its lack of particle-hole symmetry (PHS), which is supposed to be preserved for spin-polarized lowest Landau Levels [8]. As an alternative, the particle-hole symmetric Dirac composite fermion (DCF) theory for compressible state $\nu = 1/2$ has been recently proposed [9,10]. The DCF theory is characterized by a Berry phase of π around the composite Fermion surface, while the Berry phase for the particle-hole symmetry broken HLR theory is shown to be zero [9-12]. On the other hand, Wang et al. show that in the limit of long wavelengths and low frequencies, HLR theory and DCF theory are equivalent for predicting the properties of $\nu = 1/2$ state [13,14]. According to a recent proposal, the diffusion-dominated Nernst signals of $\nu = 1/2$ in the thermoelectric transport is proportional to the Berry phase around the composite Fermi surface. The Nernst signal of $\nu = 1/2$ is predicted to be non-zero with linear temperature dependence for the particle-hole symmetric case, and zero for the particle-hole symmetry (PHS) broken case [15]. Therefore, measurements of Nernst signals at $\nu = 1/2$ provide a sensitive experimental method for studying the PHS of $\nu = 1/2$ and extracting the Berry phase around the composite Fermi surface. We note that,

in thermoelectric transport, the built-in electric field E and temperature gradient ∇T are related through $E = S\nabla T$ at thermal equilibrium, where S is the Seebeck coefficient. Under external perpendicular magnetic fields, the proportionality coefficient S becomes a tensor; the off-diagonal coefficient S_{xy} is Nernst coefficient, and the diagonal coefficient S_{xx} is thermopower.

In our previous experimental work [16], the electron-diffusion dominant Nernst coefficient S_{xy}^d of $\nu = 1/2$ was measured to be very close to zero (within the noise level) in an ultra-high mobility two-dimensional electron system of GaAs/Al_xGa_{1-x}As heterostructure [16]. One challenge in studying the electron-diffusion S_{xy}^d in the GaAs/Al_xGa_{1-x}As system is that S_{xy}^d prevails over the phonon drag contributions S_{xy}^g only at very low temperatures (below 130 mK in our previous study), because the electron-phonon coupling in GaAs-based materials remains strong even at very low temperatures due to the piezoelectric effect [17]. Furthermore, at very low temperatures, the thermoelectric signal is in general very small. Therefore, it is appealing to perform similar thermal transport experiments in another material system where the diffusion-dominated regime can be achieved at higher temperatures. Unlike the piezoelectric material GaAs, the electron-phonon coupling in the Si system is mainly via the deformation potential [17-19]. The phonon drag contribution can be significantly suppressed in Si at about 1 K [17-19]. Moreover, decent integer and fractional quantum Hall effects have been observed in high-mobility SiGe heterostructures [20-22]. Considering that the electron effective mass in Si is larger than the hole effective mass in Ge, the fractional quantum Hall states in p -type

Ge/SiGe heterostructures can be observed at relatively higher temperatures [20-22].

Based on the foregoing notion, it is compelling to perform Nernst signal measurements of $\nu = 1/2$ in a Ge/SiGe hole heterostructure.

In this paper, we report the thermopower and Nernst measurement results of $\nu = 1/2$ in two-dimensional hole systems in an undoped strained Ge/SiGe heterostructure. The diffusion-dominated thermopower S_{xx}^d at $\nu = 1/2$ shows a linear dependence on temperature below 600 mK. The effective mass $m_{CF} = (0.95 \pm 0.25) m_0$ ($B = 12$ T) of composite fermions at $\nu = 1/2$ is extracted from the linear temperature dependence, where m_0 is the free electron mass. Meanwhile, the diffusion-dominated Nernst signal S_{xy}^d of $\nu = 1/2$ is found to be close to zero.

The data presented in this paper is from a two-dimensional hole system in a high quality, undoped, enhancement mode Ge/SiGe heterostructure. Details of the growth and device fabrication of the heterostructure have been reported previously [21]. The two-dimensional hole system is capacitively induced by applying a negative voltage on the top gate. The Ge/SiGe sample used in our experiment is about 2 mm wide and 7 mm long. On the hot end of the sample, a Ti/Au heater is created by lithography and metal deposition. The 100 μm wide Hall bar geometry is defined by a Hall-bar-shaped top gate. The measurement is performed in a ^3He cryostat equipped with a 15 T superconducting magnet. To create a temperature gradient across the Hall bar, as shown in Fig. 1(a), we seal our sample into a vacuum cell made of polycarbonate, and the entire cell is immersed into the ^3He liquid. The cold end of the sample is attached to a silver rod which is thermally coupled to the ^3He liquid, while the hot end is suspended. To determine the temperature difference across the Hall bar, two calibrated

RuO₂ sensors are attached to the cold and hot ends of the sample by stycast 2850 (24 LV). Standard low-frequency AC lock-in measurement techniques are used for measurements. The measurement frequency is 17 Hz for electrical transport, while for thermoelectric transport, a lower AC frequency of $2f = 3.4$ Hz is used.

Figure 1 (b) shows the magneto-resistivity and Hall resistivity of sample with density $n = 1.65 \times 10^{11} \text{ cm}^{-2}$ and mobility $\mu = 1.5 \times 10^5 \text{ cm}^2 / \text{V.s}$ as a function of magnetic field at $T = 300 \text{ mK}$. The integer quantum hall effect $\nu = 1, 2, 3$ and fractional quantum hall effect $\nu = 2/3, 3/5$ are well resolved, indicating the high quality of the undoped Ge/SiGe heterostructure used in our experiment. Correspondingly, the thermopower S_{xx} shows (Fig. 2(a)) distinct $\nu = 1$ and $\nu = 2$ integer quantum Hall state, and also $\nu = 2/3$ and $3/5$ fractional quantum Hall state (see the inset of Fig. 2(a)). We note that, the hole density shown in Fig. 2 and Fig. 3 is about $1.45 \times 10^{11} \text{ cm}^{-2}$, slightly lower than is shown in Fig. 1. Such shifts arise from different cool down cycles for obtaining the data in electrical transport (Fig.1) and thermal transport (Figs. 2 and 3). These measurement results are consistent with previous observations [16, 23-24]. The diffusion-dominated thermopower S_{xx}^d due to the thermal diffusion of carriers is proportional to the entropy of the carriers (quasiparticles) [25, 26]. Hence, the S_{xx}^d is maximum when the chemical potential μ is in the extended states of Landau levels, where the entropy of carriers is at a maximal value. The S_{xx}^d is at a minimal value when the chemical potential μ is tuned into the gap between Landau levels. The phonon-drag thermopower S_{xx}^g , on the other hand, arises from the thermal transport of carriers that gain momentum from phonons.

Carriers in the extended states are more likely to be scattered by phonons than carriers in the localized states between Landau levels. As such, both S_{xx}^d and S_{xx}^g as a function of magnetic field exhibit the same oscillations, which are in phase with the oscillations of longitudinal magneto-resistivity R_{xx} as well.

Figure 2(b) illustrates the temperature dependence of thermopower S_{xx}^d at $\nu = 1/2$. In HLR theory, the $\nu = 1/2$ state can be regarded as quasiparticles effectively in a zero magnetic field. The temperature dependence of thermopower S_{xx} at $\nu = 1/2$ is therefore similar to that of S_{xx} at $B = 0$ T [27]. Specifically, the phonon-drag thermopower S_{xx}^g of $\nu = 1/2$ should have a power-law temperature dependence, while the diffusion thermopower S_{xx}^d of $\nu = 1/2$ (indicated to be entropy per quasiparticle per charge) should have a linear temperature dependence [25, 27]. From the fitting results shown in Fig. 2(b), the phonon-drag thermopower (above 600 mK) S_{xx}^g shows a power law temperature dependence of $T^{2.2}$. Below 600 mK, the diffusion dominant thermopower follows a linear temperature dependence. The crossover temperature of 600 mK is similar to previously reported results [17-19] and is also much higher than that (about 100 mK) measured in GaAs-based materials [16, 23, 28]. According to theoretical predictions [27], the diffusion thermopower S_{xx}^d of $\nu = 1/2$ is given by,

$$S_{xx}^d(\nu = 1/2) = -\frac{\pi k_B^2 m_{CF} (1 + p_{CF})}{6\hbar^2 en} T, \quad (1)$$

where m_{CF} is the effective mass of composite fermions, n is the density of carriers, and p_{CF} represents the impurity scattering parameter. Based on the coefficient from the linear fit shown in Fig. 2(b), we estimate $m_{CF} \approx (0.95 \pm 0.25) m_0$ ($B = 12$ T), where m_0 is the free electron mass. Note that we take $p_{CF} = 0$ for the estimation due to the

weak energy dependence of impurity scattering. We find that the m_{CF} obtained here is in agreement with the previously reported results of $m_{CF} (\nu = 1/2) \approx 1.0m_0$, which was obtained from thermal transport measurements based on another two-dimensional hole system in a GaAs/AlGaAs heterostructure [23]. For this comparison, the difference of magnetic field at $\nu = 1/2$ has been taken into account. Overall, the properties of thermopower S_{xx} at $\nu = 1/2$ obtained from our experiment are consistent with previous reports.

The Nernst signals S_{xy} as a function of magnetic field at different temperatures are shown in Fig. 3(a). It can be seen that the magnitude of Nernst signal S_{xy} also increases with increasing temperature. The S_{xy} at $T \approx 313$ mK (inset of Fig. 3(a)) displays distinct oscillations as a function of magnetic field. According to theoretical predictions, the diffusion-dominated thermopower S_{xx}^d and Nernst S_{xy}^d for weakly disordered, non-interacting two-dimensional electrons (holes) in the quantum hall regime should follow the generalized Mott formula [27, 29-31]:

$$S_{ij}^d(\varepsilon_F, T, B) = -\frac{\pi^2 k_B^2}{3e} \rho_{ik} \left[\frac{d\sigma}{d\varepsilon} \right]_{kj} \Big|_{\varepsilon=\varepsilon_F} T, \quad (2)$$

where ε_F is the Fermi energy of electrons (holes), and ρ and σ are the electric resistivity and conductivity tensors, respectively. According to the generalized Mott formula Eq. (2), the diffusion Nernst signal S_{xy}^d in the quantum hall regime can be regarded as the derivative of entropy, which is proportional to the term of $\rho_{xy} * d\sigma_{xx} / dB + \rho_{xx} * d\sigma_{xy} / dB$. We calculate this term by using the magneto-resistivity ρ_{xx} and ρ_{xy} against magnetic fields at $T = 300$ mK, and the calculated result is qualitatively shown in the inset of Fig. 3(a) (red line). At $\nu = 1$, the

calculated term (or S_{xy}^d trace) is zero. Away from $\nu = 1$, the calculated term first shows a positive peak, then drop to zero at the position where the ρ_{xx} or σ_{xx} are maximal values, then followed by a negative peak. Considering that the fractional quantum hall effect can be regarded as the integer quantum hall effect of composite fermions, S_{xy}^d in the fractional quantum hall regime could also correspond to the same trace shape as that of S_{xy}^d near $\nu = 1$. [29-32]. Qualitatively, the oscillation of the measured Nernst signal S_{xy} at $T \approx 313$ mK in the QH regime is consistent with the shape of this calculated term, which suggests that the Nernst signal S_{xy} at $T \approx 313$ mK is indeed in the diffusion-dominated regime. Furthermore, at $\nu = 1/2$, the measured diffusion Nernst S_{xy}^d at $T \approx 313$ mK approaches zero and has the same order of magnitude with the background noise.

To better understand the behavior of Nernst signals at $\nu = 1/2$, we examined the temperature dependence of this signal. As shown in Fig. 3(b), the blue and black traces are curve fits of $a * T^n$ and $a * T + b * T^n$ to the measured Nernst signal of $\nu = 1/2$ (shown as red dots with error bar), respectively, where a , b and n are the fitting parameters. The inset of Fig. 3(b) shows the detail of the temperature dependence below the crossover temperature. Note that the uncertainty of the measured Nernst signal below the crossover temperature of 600 mK is comparable to the measured signal amplitude, allowing the measured data to be fit with the two different fitting functions shown above. From a theoretical perspective, the power law fit of $T^{2.6 \pm 0.15}$ shown in Fig. 3(b) is just for the phonon-drag contribution, but it still fits well with the measured data even in the diffusion-dominated regime. This observation suggests

that the Nernst signal of $\nu = 1/2$ from the diffusion contribution is negligible compared to the phonon-drag contribution, even below a crossover temperature of 600 mK (in the diffusion-dominated regime). One possible reason for the negligible diffusion contribution is that the PHS of $\nu = 1/2$ ($B = 12$ T) is broken in our experiment. The broken PHS may result from the Landau level mixing, which exists to some degree due to Coulomb interactions in realistic systems [9, 10, 15]. As for the other fitting function of $a*T + b*T^{3.7\pm 0.5}$, it does indeed possess a term with linear temperature dependence. However, as compared to the $a*T^n$ fitting, this more complex term shows a larger deviation from the measured data points (in general larger than the measured values), which may also indicate that the diffusion contribution is negligible here.

According to Wang et al. [33], the density of composite fermions in the Dirac composite fermion theory is proportional to the applied magnetic field, and the density of composite fermions is equal to the carrier density only at $\nu = 1/2$. Thus, the coherent Berry phase cannot be observed if sweeping the applied magnetic field during measurements, because the density and effective magnetic fields for composite fermions are changing simultaneously. Motivated by this constraint and while using the same device, we perform thermal transport measurements around $\nu = 1/2$ by changing the density (i.e. changing the front gate voltage V_f) consecutively at a fixed external magnetic field $B = 11$ T. Figure 4(a) and (b) show the thermopower S_{xx} and Nernst S_{xy} as a function of V_f at $B = 11$ T for different temperatures, respectively. Note that each trace in Fig. 4(b) is the average trace of six raw data traces measured at the

same conditions. Again, the magnitude of S_{xx} and S_{xy} increase with increasing temperatures. At the lowest temperature $T = 334$ mK, the thermopower S_{xx} shown in the inset of Fig. 4(a) displays the distinct fractional quantum hall states of $\nu = 1/3$, $2/5$, and $3/5$ around $\nu = 1/2$. The Nernst S_{xy} at $T = 334$ mK is shown as the inset of Fig. 4 (b). The shape of S_{xy} in the fractional quantum Hall effect regime is similar to that shown in Fig. 3(a), which corresponds to the derivative of the entropy, namely, the derivative of thermopower S_{xx} . For $\nu = 1/2$, the S_{xy} is still very close to zero. In short, all of these features of S_{xx} and S_{xy} are qualitatively similar to that observed from the conventional measurement configuration (sweeping magnetic field with fixed carrier density) [34].

In conclusion, we study the thermopower and Nernst signal of $\nu = 1/2$ of a two-dimensional hole system in a high quality undoped strained Ge/SiGe heterostructure. The crossover temperature differentiating the diffusion and phonon-drag dominated regimes is about 600 mK, which is much higher than that observed in piezoelectric, GaAs heterostructures. The diffusion-dominated thermopower S_{xx}^d at $\nu = 1/2$ shows a linear temperature dependence, which is consistent with previous observations [16, 23]. However, the diffusion-dominated Nernst signal S_{xy}^d of $\nu = 1/2$ is found to approach zero, which is independent of the measurement configuration (sweeping external magnetic field at fixed carrier density or sweeping carrier density at fixed magnetic field). Though the diffusion contribution can be dominant at a higher temperature (~ 600 mK) in the SiGe heterostructure than that (~ 100 mK) in the GaAs heterostructure, the diffusion-dominated Nernst signal at $\nu = 1/2$ is still shown to approach zero, which is similar to what we previously observed in a GaAs system [16]. One possible reason for the vanishing S_{xy}^d of $\nu = 1/2$

is that the particle-hole symmetry of $\nu = 1/2$ is broken, presumably due to Landau level mixing. In addition, it is still possible that the S_{xy}^d of $\nu = 1/2$ is non-zero but too small compared to the phonon contributions and/or background noise. More experimental studies are required to examine the conditions under which the PHS of $\nu = 1/2$ is preserved in the real system.

Acknowledgements

We acknowledge valuable help from Changli Yang. The work at Rice was funded by NSF Grant No. DMR-1508644 and Welch Foundation Grant No. C-1682. This work was performed, in part, at the Center for Integrated Nanotechnologies, a U.S. DOE, Office of Basic Energy Sciences, user facility. Sandia National Laboratories is a multimission laboratory managed and operated by National Technology and Engineering Solutions of Sandia LLC, a wholly owned subsidiary of Honeywell International Inc. for the U.S. Department of Energy's National Nuclear Security Administration under contract DE-NA0003525. The views expressed in the article do not necessarily represent the views of the U.S. Department of Energy or the United States Government. The work at National Taiwan University has been supported by the Ministry of Science and Technology (106-2112-M-002-009-, 107-2218-E-002-044 and 107-2622-8-002-018) and the Ministry of Education (NTU-CC-108L891701, NTU-107L7818, and NTU-107L891702).

Reference

- [1] B. I. Halperin, P. A. Lee, and N. Read, *Theory of the Half-Filled Landau Level*, Phys. Rev. B **47**, 7312 (1993).
- [2] J. K. Jain, *Composite-Fermion Approach for the Fractional Quantum Hall Effect*, Phys. Rev. Lett. **63**, 199 (1989).
- [3] R. L. Willett, R. R. Ruel, K. W. West, and L. N. Pfeiffer, *Experimental Demonstration of a Fermi Surface at One-Half Filling of the Lowest Landau Level*, Phys. Rev. Lett. **71**, 3846 (1993).
- [4] R. L. Willett, M. A. Paalanen, R. R. Ruel, K. W. West, L. N. Pfeiffer, and D. J. Bishop, *Anomalous Sound Propagation at $\nu = 1/2$ in a 2D Electron Gas: Observation of a Spontaneously Broken Translational Symmetry?*, Phys. Rev. Lett. **65**, 112 (1990).
- [5] V. J. Goldman, B. Su, and J. K. Jain, *Detection of Composite Fermions by Magnetic Focusing*, Phys. Rev. Lett. **72**, 2065 (1994).
- [6] D. Kamburov, M. Shayegan, L. N. Pfeiffer, K. W. West, and K. W. Baldwin, *Commensurability Oscillations of Hole-Flux Composite Fermions*, Phys. Rev. Lett. **109**, 236401 (2012).
- [7] D. Kamburov, Yang Liu, M. A. Mueed, M. Shayegan, L. N. Pfeiffer, K. W. West, and K. W. Baldwin, *What Determines the Fermi Wave Vector of Composite Fermions?*, Phys. Rev. Lett. **113**, 196801 (2014).
- [8] S. M. Girvin, *Particle-hole symmetry in the anomalous quantum Hall effect*, Phys. Rev. B **29**, 6012 (1984).
- [9] Dam Thanh Son, *Is the composite fermion a Dirac particle?*, Phys. Rev. X **5**, 031027 (2015).
- [10] Dam Thanh Son, *The Dirac composite fermion of the fractional quantum Hall effect*, Prog. Theor. Exp. Phys. **2016**, 12C103 (2016). Michael Levin and Dam Thanh Son, *Particle-hole symmetry and electromagnetic response of a half-filled Landau level*, Phys. Rev. B **95**, 125120 (2017).
- [11] Scott D. Geraedts, Michael P. Zaletel, Roger S. K. Mong, Max A. Metlitski, Ashvin Vishwanath, Olexei I. Motrunich, *The half-filled Landau level: The case for Dirac composite fermions*, Science **352**, 197 (2016).

- [12] Chong Wang, T. Senthil, *Half-filled Landau level, topological insulator surfaces, and three dimensional quantum spin liquids*, Phys. Rev. B **93**, 085110 (2016).
- [13] Chong Wang, Nigel R. Cooper, Bertrand I. Halperin, and Ady Stern, *Particle-Hole Symmetry in the Fermion-Chern-Simons and Dirac Descriptions of a Half-Filled Landau Level*, Phys. Rev. X **7**, 031029 (2017).
- [14] Alfred K. C. Cheung, S. Raghu, and Michael Mulligan, *Weiss oscillations and particle-hole symmetry at the half-filled Landau level*, Phys. Rev. B **95**, 235424 (2016).
- [15] Andrew C. Potter, Maksym Serbyn, and Ashvin Vishwanath, *Thermoelectric Transport Signatures of Dirac Composite Fermions in the Half-Filled Landau Level*, Phys. Rev. X **6**, 031026 (2016).
- [16] Xiaoxue Liu, Tingxin Li, Po Zhang, L. N. Pfeiffer, K. W. West, Chi Zhang, and Rui-Rui Du, *Thermopower and Nernst measurements in a half-filled lowest Landau level*, Phys. Rev. B **97**, 245425 (2018).
- [17] R Fletcher, *Magnetothermoelectric effects in semiconductor systems*, Semicond. Sci. Technol. **14**, R1–R15 (1999).
- [18] C. Possanzini, R. Fletcher, M. Tsaousidou, P. T. Coleridge, R. L. Williams, Y. Feng, and J. C. Maan, *Thermopower of a p-type Si/Si_{1-x}Ge_x heterostructure*, Phys. Rev. B **69**, 195306 (2004).
- [19] C. Possanzini, R. Fletcher, P.T. Coleridge, Y. Feng, R. L. Williams, and J.C. Maan, *Diffusion Thermopower of a Two-Dimensional Hole Gas in SiGe in a Quantum Hall Insulating State*, Phys. Rev. Lett. **90**.176601(2003).
- [20] T. M. Lu, D. C. Tsui, C.-H. Lee, and C. W. Liu, *Observation of two-dimensional electron gas in a Si quantum well with mobility of 1.6×10^6 cm²/V.s*, Appl. Phys. Lett, **94**, 182102 (2009).
- [21] D. Laroche, S.-H. Huang, Y. Chuang, J.-Y. Li, C.W. Liu, and T. M. Lu, *Magneto-transport analysis of an ultra-low-density two-dimensional hole gas in an undoped strained Ge/SiGe heterostructure*, Appl. Phys. Lett, **108**, 233504 (2016).
- [22] T.M. Lu, W. Pan, D. C. Tsui, C.-H. Lee, and C.W. Liu, *Fractional quantum Hall effect of two-dimensional electrons in high-mobility Si/SiGe field-effect transistors*, Phys. Rev. B **85**, 121307(R) (2012).
- [23] X. Ying, V. Bayot, M. B. Santos and M. Shayegan, *Observation of composite-fermion thermopower at half-filled Landau levels*, Phys. Rev. B **50**, 4969 (1994).
- [24] V. Bayot, E. Grivei, H. C. Manoharan, X. Ying and M. Shayegan, *Thermopower*

- of composite fermions*, Phys. Rev. B **52**, R8621 (1995).
- [25] M. Cutler and N. F. Mott, *Observation of Anderson Localization in an Electron Gas*, Phys. Rev, **181**, 1336 (1968).
- [26] M. Jonson, S. M. Girvin, *Thermoelectric effect in a weakly disordered inversion layer subject to a quantizing magnetic field*, Phys. Rev. B **29**, 1939 (1984).
- [27] N. R. Cooper, B. I. Halperin, and I. M. Ruzin, *Thermoelectric response of an interacting two-dimensional electron gas in a quantizing magnetic field*, Phys. Rev. B **55**, 2344 (1997).
- [28] W. E. Chickering, J. P. Eisenstein, L. N. Pfeiffer, and K. W. West, *Thermopower of two-dimensional electrons at filling factors $\nu = 3/2$ and $5/2$* , Phys. Rev. B **81**, 245319 (2010).
- [29] Herbert Oji, *Thermopower and thermal conductivity in two-dimensional systems in a quantizing magnetic field*, Phys. Rev. B **29**, 3148 (1984).
- [30] R. Fletcher, J.C. Maan, K. Ploog and G. Weimann, *Thermoelectric properties of GaAs-Ga_{1-x}Al_xAs heterojunctions at high magnetic fields*, Phys. Rev. B **33**, 7122 (1985).
- [31] R. Shirasaki, A. Endo, N. Hatano, and H. Nakamura, *Thermomagnetic Effect in the Quantum Hall System*, Journal of electronic materials **41**, 1540 (2012).
- [32] V. C. Karavolas, G. P. Triberis and F. M. Peeters, *Electrical and thermal transport of composite fermions*, Phys. Rev. B **56**, 15289 (1997).
- [33] Wang, C. & Senthil, T. *Composite Fermi liquids in the lowest Landau level*. Phys. Rev. B **94**, 245107 (2016).
- [34] See Supplemental Material at for the temperature dependence of S_{xx} and S_{xy} at $\nu = 1/2$ in the gate-swept configuration.

Figures

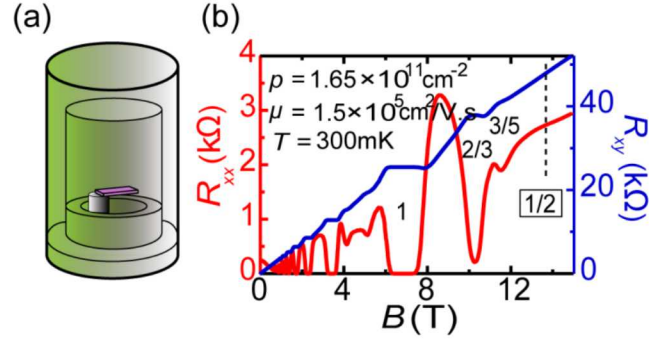


Fig. 1. (a) An illustration of the experimental setup, showing the Hall bar sample cantilevered to a heat sink and surrounded by a vacuum shield. (b) The longitudinal and Hall resistivity as a function of magnetic field at $T = 300$ mK. The hole density and mobility are labeled in the figure.

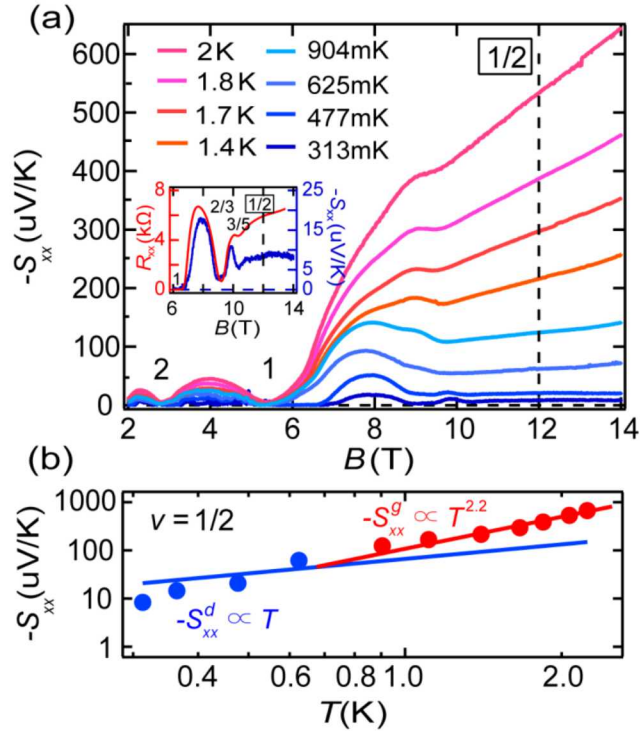


Fig. 2. (a) The thermopower S_{xx} as a function of magnetic field at different temperatures. The thermopower S_{xx} near $\nu = 1/2$ at $T = 313$ mK along with the corresponding longitudinal resistivity R_{xx} are shown in the inset. (b) The temperature dependence of thermopower S_{xx} at $\nu = 1/2$. The blue and red traces are the fit to the measured data in the diffusion-dominated regime (blue circles with error bars) and phonon-drag dominated regime (red circles), respectively. The error bar scale is below the size of the blue circles. The diffusion thermopower S_{xx}^d shows

a linear temperature dependence, while the phonon-drag thermopower S_{xx}^g shows a power law temperature dependence of $T^{2.2}$.

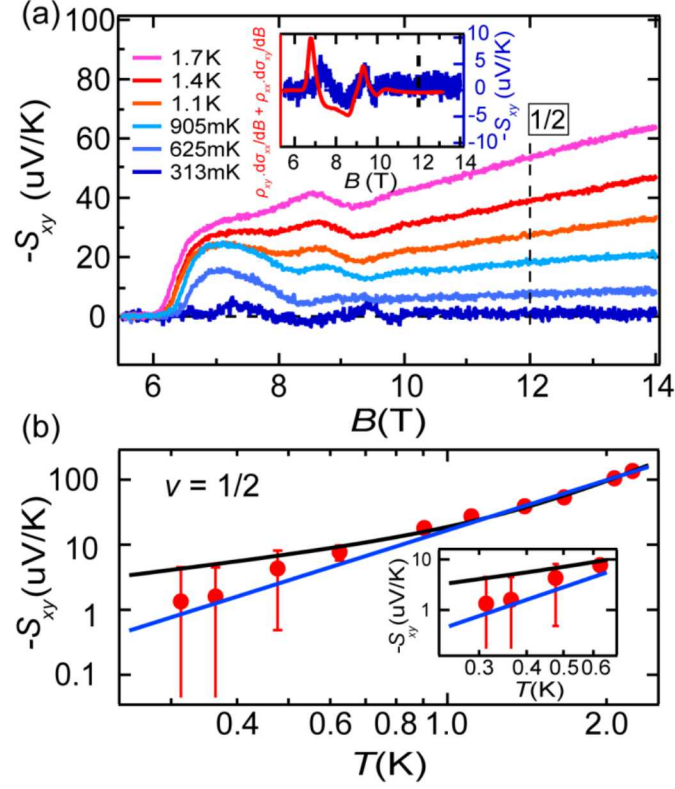


Fig. 3. (a) The Nernst signal S_{xy} as a function of magnetic fields at different temperatures. The Nernst signal S_{xy} near $\nu = 1/2$ at $T = 313$ mK along with the calculated $\rho_{xy} \cdot d\sigma_{xx}/dB + \rho_{xx} \cdot d\sigma_{xy}/dB$ are shown in the inset. (b) The temperature dependence of Nernst signal S_{xy} at $\nu = 1/2$. The blue trace is the power fit of $T^{2.6 \pm 0.15}$ and the black trace is the fit of $aT + bT^{3.7 \pm 0.5}$ to the measured S_{xy} at $\nu = 1/2$ shown as red circles with error bars, respectively. The inset shows the detailed view of S_{xy} at $\nu = 1/2$ as a function of temperature below $T < 700$ mK.

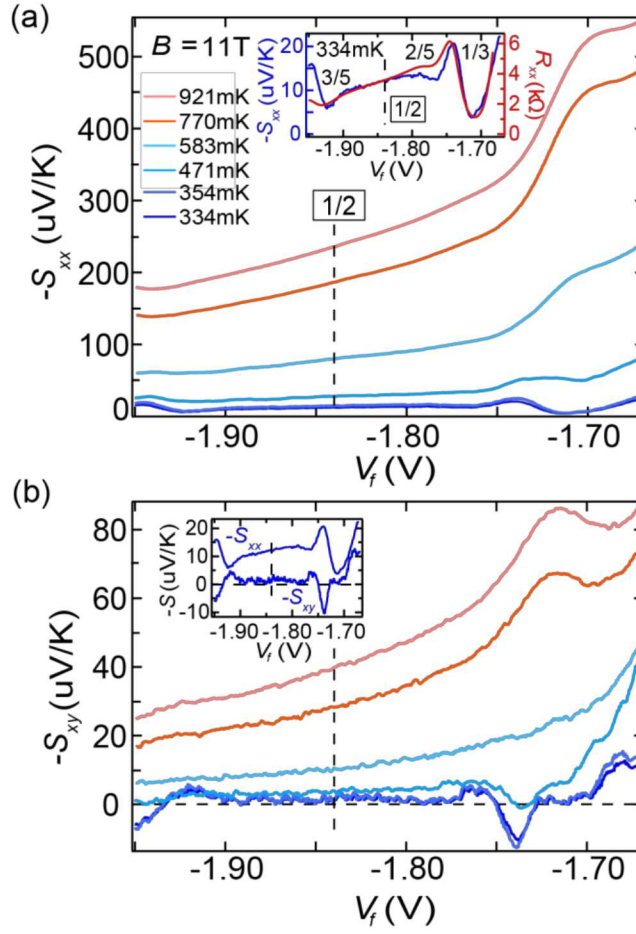


Fig. 4 (a) (b) The thermopower $-S_{xx}$ and Nernst signals $-S_{xy}$ as a function of front gate V_f at $B = 11$ T at different temperatures. The different temperatures are shown in (a). The inset in (a) shows the thermopower $-S_{xx}$ at $T = 334$ mK along with the longitudinal resistivity R_{xx} vs V_f at $B = 11$ T. The inset in (b) shows Nernst S_{xy} and thermopower S_{xx} at $T = 334$ mK as a function of V_f at $B = 11$ T. The $\nu = 1/2$ is labeled by vertical black dashed line in (a) and (b).